AIP | Applied Physics Letters

# Electronic, transport, and optical properties of bulk and mono-layer PdSe2

Jifeng Sun, Hongliang Shi, Theo Siegrist, and David J. Singh

Citation: Applied Physics Letters **107**, 153902 (2015); doi: 10.1063/1.4933302
View online: http://dx.doi.org/10.1063/1.4933302
View Table of Contents: http://scitation.aip.org/content/aip/journal/apl/107/15?ver=pdfcov
Published by the AIP Publishing

**Articles you may be interested in**

Thermoelectric transport coefficients in mono-layer MoS2 and WSe2: Role of substrate, interface phonons, plasmon, and dynamic screening
J. Appl. Phys. **118**, 135711 (2015); 10.1063/1.4932140

The elastic and thermoelectric properties of the Zintl compound Ca5Al2Sb6 under high pressure
J. Appl. Phys. **116**, 223709 (2014); 10.1063/1.4902949

Electronic and transport properties of zintl phase AeMg2Pn2, Ae=Ca,Sr,Ba, Pn=As,Sb,Bi in relation to Mg3Sb2
J. Appl. Phys. **114**, 143703 (2013); 10.1063/1.4824465

Mechanically strained tuning of the electronic and dielectric properties of monolayer honeycomb structure of tungsten disulphide(WS2)
AIP Conf. Proc. **1512**, 1242 (2013); 10.1063/1.4791501

Electronic structure and optical conductivity of two dimensional (2D) MoS2: Pseudopotential DFT versus full potential calculations
AIP Conf. Proc. **1447**, 1269 (2012); 10.1063/1.4710474

This article is copyrighted as indicated in the article. Reuse of AIP content is subject to the terms at: http://scitation.aip.org/termsconditions. Downloaded to IP: 128.219.49.14 On: Tue, 12 Jan 2016 21:14:48

# Electronic, transport, and optical properties of bulk and mono-layer $PdSe_2$

Jifeng Sun,[1,2] Hongliang Shi,[2] Theo Siegrist,[3] and David J. Singh[1,a)]
[1]*Department of Physics and Astronomy, University of Missouri-Columbia, Columbia, Missouri 65211, USA*
[2]*Materials Science and Technology Division, Oak Ridge National Laboratory, Oak Ridge, Tennessee 37831, USA*
[3]*Department of Chemical and Biomedical Engineering, College of Engineering, Florida Agricultural and Mechanical University-Florida State University, 2525 Pottsdamer St., Tallahassee, Florida 32310, USA*

(Received 9 July 2015; accepted 5 October 2015; published online 13 October 2015)

The electronic and optical properties of bulk and monolayer $PdSe_2$ are investigated using first-principles calculations. Using the modified Becke-Johnson potential, we find semiconductor behavior for both bulk and monolayer $PdSe_2$ with indirect gap values of 0.03 eV for bulk and 1.43 eV for monolayer, respectively. Our sheet optical conductivity results support this observation and show similar anisotropic feature in the 2D plane. We further study the thermoelectric properties of the 2D $PdSe_2$ using Blotzmann transport model and find interestingly high Seebeck coefficients ($>200\,\mu V/K$) for both *p*- and *n*-type up to high doping level ($\sim 2 \times 10^{13}\,cm^{-2}$) with an anisotropic character in an electrical conductivity suggesting better thermoelectric performance along *y* direction in the plane. © *2015 AIP Publishing LLC*. [http://dx.doi.org/10.1063/1.4933302]

Layered transition metal di-chalcogenides (TMDCs), especially their two-dimensional (2D) counterparts, are a class of materials with fascinating and technologically useful properties.[1,2] Depending on the stoichiometry, the three-dimensional TMDCs with a formula $MX_2$, where M represents transition metals and X is chalcogen, can be either metals or semiconductors with indirect band gaps. Whereas the 2D monolayers are direct-band-gap semiconductors with sizable bandgaps around 1–2 eV.[3] This band-gap phenomenon together with the versatile chemistry of $MX_2$ enables a variety of fields of applications including field-effect transistors, energy storage, and catalysis.[1–4]

Several TMDCs (e.g., $MoS_2$, $MoSe_2$, and $WS_2$) have been extensively investigated, both experimentally and theoretically.[5–12] However, there are not many studies on the palladium dichalcogenides ($PdX_2$). The series with X = S, Se, and Te are known to occur in bulk forms,[13–15] but no experimental evidence exists on its isolation in monolayer form. Here, in this paper we investigate $PdSe_2$ in both bulk and monolayer forms, using electronic structure and transport calculations based on density functional theory (DFT)[16,17] and Boltzmann transport theory. We compare the crystal structure, electronic structure, and optical properties between 2D monolayer and bulk $PdSe_2$, and the thermoelectric properties of 2D monolayer are also studied. The results show that both bulk and monolayer $PdSe_2$ are indirect semiconductors, with band-gap values of 0.03 eV for bulk and 1.43 eV for monolayer, respectively. We also find anisotropic character in both bulk and 2D optical conductivities. The thermoelectric properties results reveal high Seebeck coefficients for monolayer $PdSe_2$ and suggest better performance along *y* direction in the plane.

Bulk $PdSe_2$ crystallizes in a $PdS_2$-type orthorhombic structure with space group Pbca, which is shown in Fig. 1. As seen, the bulk structure is composed of 2D Se-Pd-Se layers stacking along the *c* axis which are well separated from each other with apparently van der Waals gaps. Each monolayer has a trilayer configuration with Pd atoms in the middle that are covalently bonded to four Se atoms located in the top and bottom layers. Furthermore, Se-Se bonding links the top and bottom layers. This arrangement is related to the marcasite type structure of $FeS_2$, but with larger

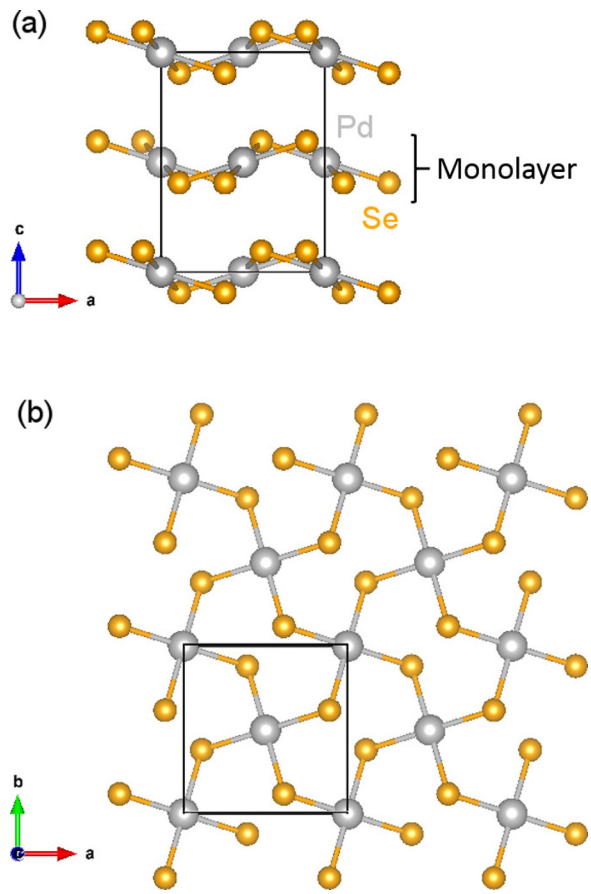


FIG. 1. Side view (a) and top view (b) of crystal structure of bulk $PdSe_2$. Solid line indicates the unit cell.

a)Electronic mail: singhdj@missouri.edu

 © 2015 AIP Publishing LLC

This article is copyrighted as indicated in the article. Reuse of AIP content is subject to the terms at: http://scitation.aip.org/termsconditions. Downloaded to IP: 128.219.49.14 On: Tue, 12 Jan 2016 21:14:48

separation of the planes. In our calculations, the monolayer structure was cut out from the bulk structure by adding vacuum space along *c* axis. It is worth noting that the structure enables potential anisotropy in the plane.

Our *ab-initio* calculations of bulk and monolayer $PdSe_2$ are performed using the linearized augmented plane-wave (LAPW) method[18] as implemented in the WIEN2K code.[19] We started from the experimental bulk structure with $a = 5.7457$ Å, $b = 5.8659$ Å, and $c = 7.6946$ Å.[14] Then the general gradient approximation (GGA) of Perdew-Burke-Ernzerhof (PBE) functional[20] was used to relax the internal coordinates for both bulk and monolayer structures. The calculated total energy of $PdSe_2$ was 280 meV per formula unit (f.u.) higher for 2D structure comparing to bulk within PBE. This energy difference increased to 570 meV/f.u. when the van der Waals interaction is considered using the DFT-D3 functional.[21] Reported layer binding energies for graphite (~35 meV/atom),[22] h-BN (52 meV/atom),[23] and black phosphorous (40 meV/atom),[23] which are the basis of the important 2D materials are smaller than that obtained for $PdSe_2$ (190 meV/atom). Common methods for preparing 2D layers are mechanical exfoliation, layer by layer growth on a substrate, e.g., by chemical vapor or physical deposition, and solvent exfoliation.[24,25] The relatively high layer binding energy may suggest difficulties in making monolayer $PdSe_2$ using mechanical exfoliation comparing to above 2D materials but other methods might be applicable. The modified Becke-Johnson[26] (mBJ) potential was employed in the calculations of electronic, optical, and transport properties because the energy gaps computed using mBJ are substantially better than GGA-PBE and other functionals in a variety of semiconductors and insulators.[27–30] The LAPW sphere radii were 2.5 Bohr for Pd and 2.1 Bohr for Se and the cut-off parameter for the basis was $R_{min}K_{max} = 7$. Experimental lattice constants[14] were used and the atomic coordinates were fully optimized by minimizing the forces down to 1 mRy/a.u. for both bulk and monolayer structures. A vacuum slab about 15 Å is added in the direction perpendicular to the nano-sheet plane for the monolayer calculations. The self-consistent calculations were performed with a $5 \times 5 \times 3$ *k*-point mesh for bulk and $7 \times 7 \times 1$ for monolayer, respectively. The density of states (DOS) and optical properties are calculated in denser *k* meshes with a value of $23 \times 23 \times 17$ for bulk and $40 \times 40 \times 1$ for monolayer. The thermopower was analysed using the Boltztrap code[31] employing Boltzmann transport theory within the constant scattering time approximation (CSTA). This CSTA approach has been shown to be successful in calculating the Seebeck coefficient in a variety of thermoelectric materials.[27,28,32,33] Importantly, the main assumption of CSTA that the energy dependence of the scattering rate is negligible compared with the energy dependence of the electronic structure, does not imply any assumption about the temperature or doping dependence of the scattering rate. A more detailed description of this approach can be found elsewhere.[32,34] We used 10 000*k* points in the Brillouin zone for calculating the transport properties. Spin-orbit coupling is included in all the calculations, except structure relaxations.

The electronic DOS for both bulk and monolayer $PdSe_2$ are shown in Fig. 2. It is clear that both bulk and monolayer

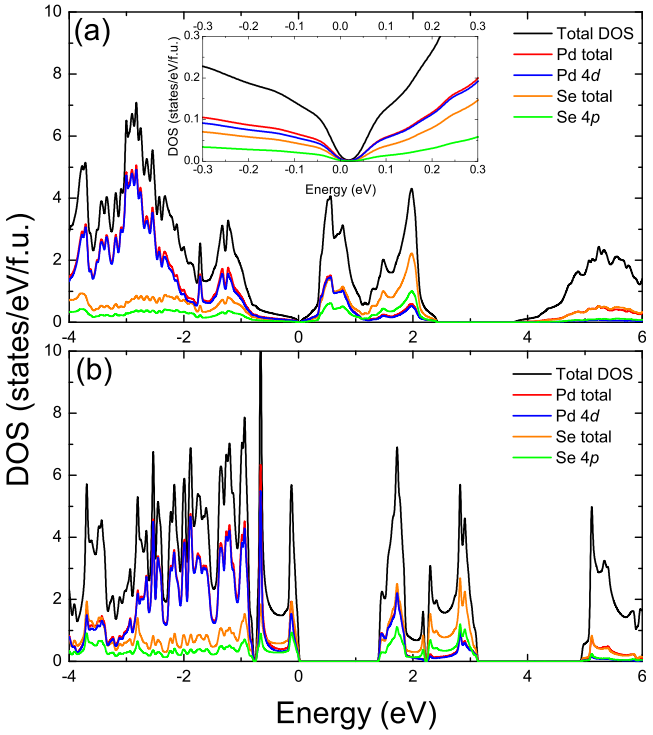


FIG. 2. Calculated density of states of $PdSe_2$ in both bulk (a) and monolayer (b). The Fermi energy is set to zero for both cases.

phases exhibit band gaps with a value of 0.03 eV for bulk and 1.43 eV for monolayer, respectively. We also did calculations for the 2D system with 1% uniform compression and expansion of the in-plane lattice parameters, again relaxing the atomic positions. With the GGA-PBE functional including spin-orbit we find that the band gap increases under compression and changes by 0.14 eV between the compressed and expanded case. This can be viewed as an error bar for the effect of typical DFT errors on the structure. It also indicates a potentially useful possibility for strain tuning with areal deformation potential of −3.5 eV.

The 2D band gap of $PdSe_2$ is in agreement with the report of Lebègue and coworkers,[15] where the PBE-GGA was used without spin-orbit coupling. From the projected DOS, the *d*-states of transition metal atoms and *p*-states of selenium atoms contribute most to the states at both valence band edge and conduction band edge for both cases. There is clear hybridization between Pd 4*d* states and Se 4*p* states that originates from the covalent bonding in the Se-Pd-Se layers, which is similar to $MoS_2$ and other TMDCs. Fig. 3 depicts the calculated band structures along high symmetry *k*-points. As seen, we find indirect band gaps in both structures. The finding in the bulk case is in contrast with previous DFT study of Hamidani and coworkers who found metallic behavior using the traditional PBE-GGA functional.[13] Though with mBJ we can get a semiconductor character, our calculated band gap is still underestimated that can be seen from the fact that bulk $PdSe_2$ is experimentally a semiconductor with a 0.4 eV band gap.[35] The band-gap change within the two phases may suggest the possibility to tune the band gap of $PdSe_2$ by means of the quantum confinement.

We have also studied the optical properties of the two structures and the optical conductivity results are shown in

This article is copyrighted as indicated in the article. Reuse of AIP content is subject to the terms at: http://scitation.aip.org/termsconditions. Downloaded to IP: 128.219.49.14 On: Tue, 12 Jan 2016 21:14:48

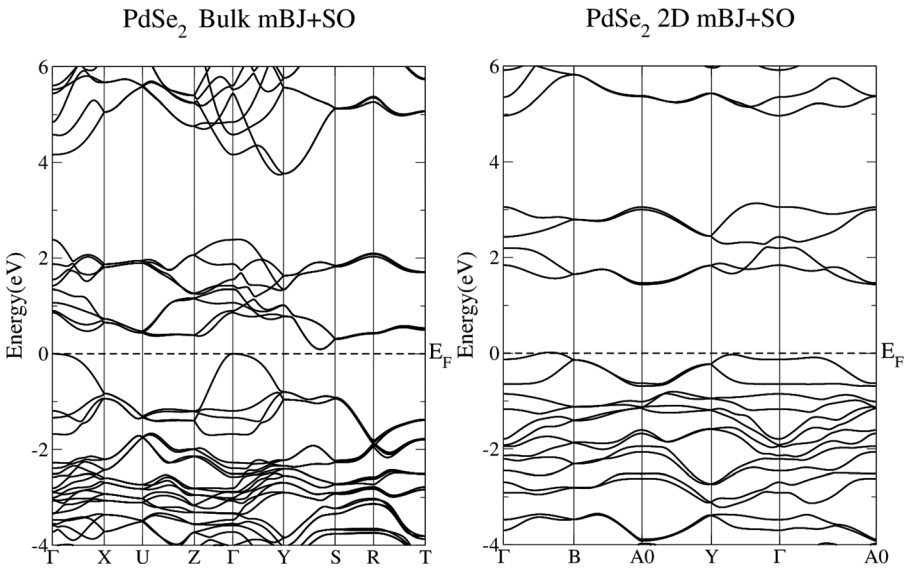


FIG. 3. Band structures of bulk $PdSe_2$ and its monolayer. The Fermi energy is set at zero for both cases.

Fig. 4. In the monolayer case, we show the sheet optical conductivity that in the van der Waals plane. As seen, the in-plane optical conductivities for both bulk and monolayer cases show a moderate anisotropic character starting from 1.5 eV for bulk structure and 1.25 eV for 2D structure, respectively. It is also noted that there is a large anisotropy in the bulk structure at energy above 1.7 eV.

Experimental studies have demonstrated that the thermoelectric properties of different 2D materials, namely, $Bi_2Te_3$ and $Bi_2Se_3$, were improved with the reducing of their thickness.[36,37] Moreover, several previous experiments on $MoS_2$ thin films and disordered layered $WSe_2$ have also demonstrated very low thermal conductivities.[38,39] Therefore, it would be interesting to study the thermoelectric properties in monolayer $PdSe_2$. Our calculated Seebeck coefficient as a function of carrier concentration at two different temperatures in the van der Waals plane is shown in Fig. 5. Substantial high Seebeck coefficients with value larger than 200 $\mu$V/K can be found in both *p*-type and *n*-type cases, at both temperatures with doping concentrations up to $2 \times 10^{13}$ cm$^{-2}$ for *p*-type and $2.5 \times 10^{13}$ cm$^{-2}$ for *n*-type. The corresponding bulk doping levels are $5.2 \times 10^{20}$ cm$^{-3}$ (with respect to the volume of bulk unit cell) and $6.5 \times 10^{20}$ cm$^{-3}$, respectively. We also note a weak anisotropic character in *p*-type Seebeck coefficient with *y* direction exhibiting better performance in the plane, whereas the *n*-type monolayer shows an almost isotropic behavior. In addition, the Seebeck coefficient tends to increase with the increasing of temperature, for both *n*- and *p*-type. Therefore, higher doping concentrations can be expected at higher temperatures. This large Seebeck at reasonable doping level is a consequence of the anisotropy of the electronic structure, which can be attributed to the density of states near the band edges. In contrast to the Seebeck coefficient, the electrical conductivity undergoes an opposite trend (shown in Fig. 6). It is clear that a relatively big electrical conductivity difference exists in the *n*-type case covering overall the doping concentration with the electrical

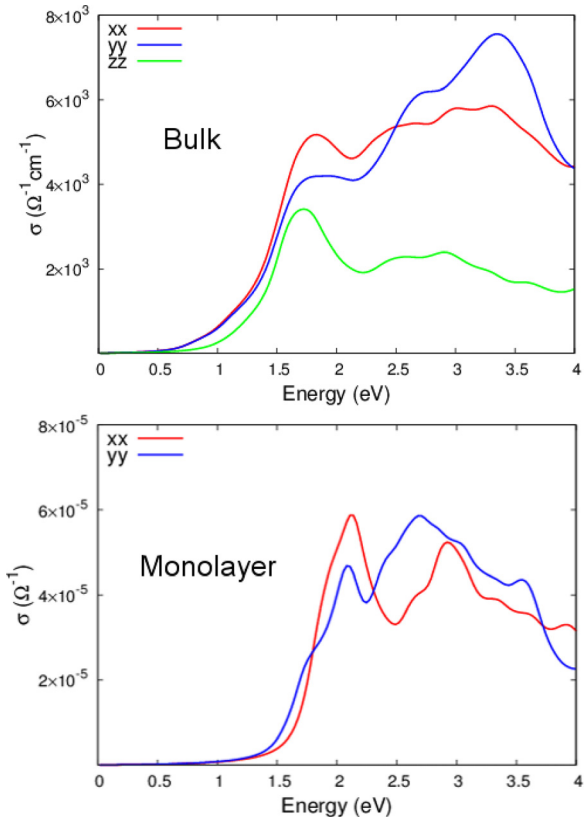


FIG. 4. Calculated optical conductivity of bulk and monolayer structures.

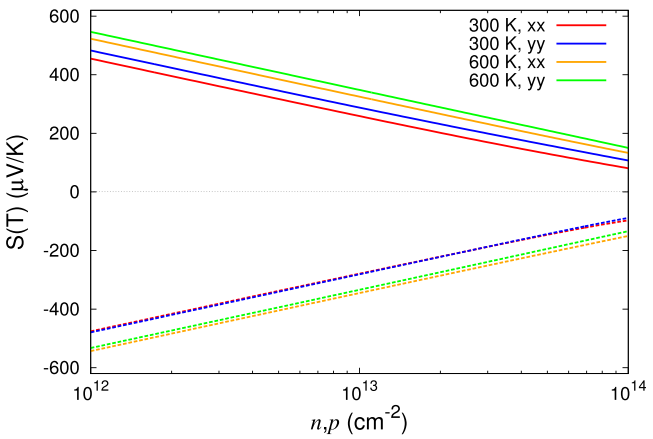


FIG. 5. Seebeck coefficients of monolayer $PdSe_2$ at 300 K and 600 K.

This article is copyrighted as indicated in the article. Reuse of AIP content is subject to the terms at: http://scitation.aip.org/termsconditions. Downloaded to IP: 128.219.49.14 On: Tue, 12 Jan 2016 21:14:48

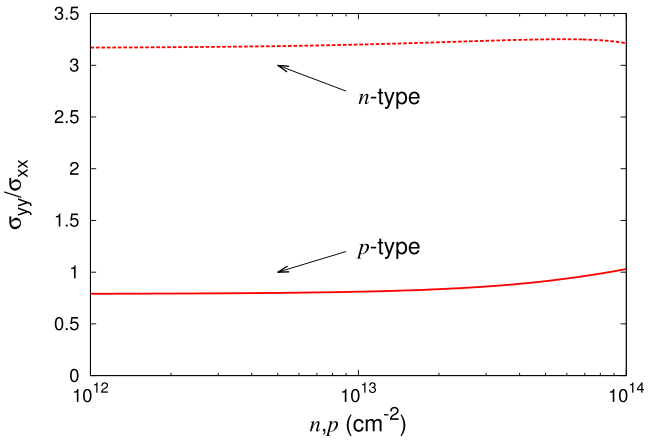


FIG. 6. Ratio of calculated electrical conductivity of monolayer $PdSe_2$ within the plane at 300 K.

conductivity in *y* direction about 3.2 times larger than *x* direction. On the other hand, for *p*-type monolayer, electrical conductivity in *y* direction is smaller with about 0.75 the value of that in *x* direction. These results may suggest potential better thermoelectric performance in *y* direction for *n*-type 2D $PdSe_2$.

In summary, we have studied the electronic and optical properties of the transition metal dichalcogenide, $PdSe_2$, in both bulk and monolayer forms using mBJ functional with spin-orbit coupling. The thermoelectric properties of the monolayer structure are also investigated within the framework of Boltzmann transport theory. We find semiconductor character in bulk and monolayer structures. The optical conductivity results indicate similar anisotropic character in the van der Waals plane in the 2D structure comparing to the bulk. Thermoelectric property calculations show substantial large Seebeck coefficients ($>200\,\mu$V/K) for both *p*- and *n*-type up to high doping level ($\sim 2\times10^{13}\,\mathrm{cm}^{-2}$). Better thermoelectric performance along *y* direction in *n* type monolayer $PdSe_2$ can be expected due to the high Seebeck coefficient and anisotropy of electrical conductivity. It will be of interest to explore the possibility of producing monolayer $PdSe_2$ and its optical and electronic properties.

This work was supported by the Department of Energy through the S3TEC Energy Frontier Research Center. J.S. acknowledges a graduate student fellowship, funded by the Department of Energy, Basic Energy Science, Materials Sciences and Engineering Division, through the ORNL GO! Program. A portion of this work was performed at the high-performance computing center at the National High Magnetic Field Laboratory.

[1]Q. H. Wang, K. Kalantar-Zadeh, A. Kis, J. N. Coleman, and M. S. Strano, Nat. Nanotechnol. **7**, 699 (2012).
[2]D. Jariwala, V. K. Sangwan, L. J. Lauhon, T. J. Marks, and M. C. Hersam, ACS Nano **8**, 1102 (2014).
[3]M. Chhowalla, H. S. Shin, G. Eda, L.-J. Li, K. P. Loh, and H. Zhang, Nat. Chem. **5**, 263 (2013).
[4]P. Miro, M. Audiffred, and T. Heine, Chem. Soc. Rev. **43**, 6537 (2014).
[5]S. Z. Butler, S. M. Hollen, L. Cao, Y. Cui, J. A. Gupta, H. R. Gutirrez, T. F. Heinz, S. S. Hong, J. Huang, A. F. Ismach *et al.*, ACS Nano **7**, 2898 (2013).
[6]H. Shi, H. Pan, Y.-W. Zhang, and B. I. Yakobson, Phys. Rev. B **87**, 155304 (2013).
[7]C. Lee, J. Hong, M.-H. Whangbo, and J. H. Shim, Chem. Mater. **25**, 3745 (2013).
[8]A. Kuc, N. Zibouche, and T. Heine, Phys. Rev. B **83**, 245213 (2011).
[9]W. Li, C. F. J. Walther, A. Kuc, and T. Heine, J. Chem. Theory Comput. **9**, 2950 (2013).
[10]W. Huang, H. Da, and G. Liang, J. Appl. Phys. **113**, 104304 (2013).
[11]E. S. Kadantsev and P. Hawrylak, Solid State Commun. **152**, 909 (2012).
[12]D. Wickramaratne, F. Zahid, and R. K. Lake, J. Chem. Phys. **140**, 124710 (2014).
[13]A. Hamidani, B. Bennecer, and K. Zanat, J. Phys. Chem. Solids **71**, 42 (2010).
[14]C. Soulard, X. Rocquefelte, P.-E. Petit, M. Evain, S. Jobic, J.-P. Iti, P. Munsch, H.-J. Koo, and M.-H. Whangbo, Inorg. Chem. **43**, 1943 (2004).
[15]S. Lebègue, T. Björkman, M. Klintenberg, R. M. Nieminen, and O. Eriksson, Phys. Rev. X **3**, 031002 (2013).
[16]P. Hohenberg and W. Kohn, Phys. Rev. B **136**, B864 (1964).
[17]W. Kohn and L. Sham, Phys. Rev. **140**, A1133 (1965).
[18]D. J. Singh and L. Nordstrom, *Planewaves, Pseudopotentials and the LAPW Method*, 2nd ed. (Springer, Berlin, 2006).
[19]K. Schwarz, P. Blaha, and G. Madsen, Comput. Phys. Commun. **147**, 71 (2002).
[20]J. P. Perdew, K. Burke, and M. Ernzerhof, Phys. Rev. Lett. **77**, 3865 (1996).
[21]S. Grimme, J. Antony, S. Ehrlich, and H. Krieg, J. Chem. Phys. **132**, 154104 (2010).
[22]L. X. Benedict, N. G. Chopra, M. L. Cohen, A. Zettl, S. G. Louie, and V. H. Crespi, Chem. Phys. Lett. **286**, 490 (1998).
[23]Y. Wang, Y. Li, and Z. Chen, J. Mater. Chem. C **3**, 9603 (2015).
[24]J. N. Coleman, M. Lotya, A. ONeill, S. D. Bergin, P. J. King, U. Khan, K. Young, A. Gaucher, S. De, R. J. Smith *et al.*, Science **331**, 568 (2011).
[25]G. Cunningham, M. Lotya, C. S. Cucinotta, S. Sanvito, S. D. Bergin, R. Menzel, M. S. P. Shaffer, and J. N. Coleman, ACS Nano **6**, 3468 (2012).
[26]F. Tran and P. Blaha, Phys. Rev. Lett. **102**, 226401 (2009).
[27]D. J. Singh, Phys. Rev. B **76**, 085110 (2007).
[28]D. Parker and D. J. Singh, Phys. Rev. B **82**, 035204 (2010).
[29]J. Sun, H. Shi, M.-H. Du, T. Siegrist, and D. J. Singh, J. Appl. Phys. **117**, 195705 (2015).
[30]J. Sun, S. Mukhopadhyay, A. Subedi, T. Siegrist, and D. J. Singh, Appl. Phys. Lett. **106**, 123907 (2015).
[31]G. Madsen and D. J. Singh, Comput. Phys. Commun. **175**, 67 (2006).
[32]D. Parker and D. J. Singh, Phys. Rev. X **1**, 021005 (2011).
[33]Y. Wang, X. Chen, T. Cui, Y. Niu, Y. Wang, M. Wang, Y. Ma, and G. Zou, Phys. Rev. B **76**, 155127 (2007).
[34]L. Zhang and D. J. Singh, Phys. Rev. B **80**, 075117 (2009).
[35]J. Wilson and A. Yoffe, Adv. Phys. **18**, 193 (1969).
[36]Y. Sun, H. Cheng, S. Gao, Q. Liu, Z. Sun, C. Xiao, C. Wu, S. Wei, and Y. Xie, J. Am. Chem. Soc. **134**, 20294 (2012).
[37]V. Goyal, D. Teweldebrhan, and A. A. Balandin, Appl. Phys. Lett. **97**, 133117 (2010).
[38]V. Varshney, S. S. Patnaik, C. Muratore, A. Roy, A. A. Voevodin, and B. L. Farmer, Comput. Mater. Sci. **48**, 101 (2010).
[39]C. Chiritescu, D. G. Cahill, N. Nguyen, D. Johnson, A. Bodapati, P. Keblinski, and P. Zschack, Science **315**, 351 (2007).

This article is copyrighted as indicated in the article. Reuse of AIP content is subject to the terms at: http://scitation.aip.org/termsconditions. Downloaded to IP: 128.219.49.14 On: Tue, 12 Jan 2016 21:14:48